Journal of Engineering and Applied Sciences 13 (12): 4381-4386, 2018
ISSN: 1816-949X

Structural and Spectroscopic Properties of AlP Diamondoids: A DFT Study

[1]Hayder M. Abduljalil and [2]Mudar Ahmed Abdulsattar
[1]Department of Physics, College of Science, University of Babylon, Babylon, Iraq
[2]Ministry of Science and Technology, Baghdad, Iraq

Abstract: Local spin density approximation (density functional theory) is used to establish the electronic structure and spectroscopic properties of Aluminum Phosphide (AlP) nanocrystals having (1.02-1.60) nm in diameter. Surface and core parts of AlP diamondoids are studied. Inspected properties include energy gap, Highest Occupied Molecular Orbital (HOMO), Lowest Unoccupied Molecular Orbital (LUMO), cohesive energy and bond length. These properties are compared to confinement theory results. Shape fluctuations are also pointed in size variation. AlP tetramantane vibrational frequencies (IR and Raman) shows that the active region in IR is similar to but with lower intensity than Raman. Size variation of AlP molecules is so that UV-Vis optical peak changes from 282-329 nm heading towards bulk experimental 496 nm as the size of AlP molecules increases. NMR spectra of AlP diamondoids are analyzed with respect to diamondoids constituting atoms. ^{1}H-NMR shielding of AlP diamondoids shows split values. The Al-H shielding is lower in value with respect to P-H shielding. Population analysis of Natural Bond Orbitals (NBO) shows that AlP diamondoids have differences from ideal sp3 bonding of carbon diamondoids. The ratio of surface to core atoms shows that the highest ratio was equal to 1.42 in diamantane structure. This ratio declines with increasing size of molecules and it is dependent on the shape of diamondoids.

Key words: Diamondoids, DFT, nanocrystals, vibration, NBO, diamantane, increasing

INTRODUCTION

Aluminum Phosphide (AlP) is a III-V semiconductor material with a wide band gap. Typically, AlP naturally exists in the zinc blende structure. The experimentally reported energy gap is 2.45-2.5 eV for bulk AlP (Casey Jr. and Panish, 1978; Shishkin and Kresse, 2007). In the case of the semiconductor surface, the dangling surface bonds lead to surface rebuilding and in smallest clusters, there is a smallest similarity to the bulk structures. Surface passivation by hydrogen atoms removes dangling bonds. The new molecular cluster is very similar to a piece of the bulk. AlP gap is large enough to surpass other direct gaps of the III-V compound semiconductors (Vurgaftman *et al*., 2001). The conduction band minimum is situated at the X point of the brillouin zone. In recent years, AlP appealed exceptional concentration to its inclusion in AlAs/AlP and GaP/AlP heterostructures. Local spin density approximation class of Density Functional Theory (DFT-LSDA) with a 6-31G basis is used in the present work to calculate electronic structure of AlP molecules. The $AlPH_6$ and AlP cyclohexane ($Al_3P_3H_{12}$) molecules are the smallest molecules investigated in present research. Diamondoids are named according to the number of their building cages. AlP diamondoids might be created by many methods such as laser ablation or RF sputtering in hydrogen environment. Investigated AlP diamondoids in the present work include AlP diamantane ($Al_7P_7H_{20}$), AlP tetramantane ($Al_{11}P_{11}H_{28}$), AlP hexamantane ($Al_{13}P_{13}H_{30}$) and AlP octamantane ($Al_{20}P_{20}H_{42}$). Semiempirical to first principles methods is applied to AlP electronic band structure (Mujica *et al*., 2003). Density functional theory are regularly used in pseudopotential (Mujica *et al*., 1999) and all-electron methods. Bulk properties of AlP are theoretically calculated based on Hartree-Fock (Froyen and Cohen, 1983) and potential models (Jivani *et al*., 2005) with an excellent description of its structural and electronic properties. Annane *et al*. (2010) examined the electronic and spectroscopic properties of AlP using full potential linear augmented plane wave plus local orbitals method. The current research reports diamondoids nanocrystals that have the size range of 1.02-1.60 nm in diameter. In diamondoids molecules and nanocrystals, atoms are split amongst core and surface. The nearly ideal zinc blende structure that is free of surface reconstruction is obtained using diamondoids structures. Previous theoretical investigations of cubic zinc blend AlP diamondoid nanocrystals do not exist in the literature. In the current research, we study the electronic structure and spectroscopic properties of AlP diamondoid nanocrystals including vibrational, UV-Vis and NMR properties with different sizes by using a Density Functional Theory (DFT) method.

Corresponding Author: Hayder M. Abduljalil, Department of Physics, College of Science, University of Babylon, Babylon, Iraq

MATERIALS AND METHODS

Theory: Density functional theory is one of the most exploited quantum mechanical approaches to simulate molecules and materials (Valone, 2010). DFT is widely applied to problems in physics and chemistry to investigate the structure of many-electron systems. Nanocrystals are an extension of the previous applications to atoms and molecules using electron correlation corrections (Jensen, 2002). DFT derives properties of a many-electron system as a function of electron density ρ(r). It depends on one spin and three spatial coordinates for every electron assuming fixed positions of nuclei (Kim *et al*., 2011; Robert and Weitao, 1994). The electron density is defined as the probability of finding an electron (s) in a particular place and tends to zero as the distance between the electron and nucleus tends to infinity. The approach to the wave function becomes significantly more complicated mathematically as the number of particles increases (Kohanoff and Gidopoulos, 2003). The experimentally measured gap of carbon adamantane is 2.5 eV (Casey Jr. and Panish, 1978). As the size of diamondoids increases, this energy gap decreases. Our selection is to pick 6-31G basis set, since, it is a reconciliation between computational time and accuracy for large AlP diamondoids. The 6-31G basis is adequate for ground state properties, so that, we can determine the binding energy, vibrational properties, transitions and energy gap with acceptable accuracy. DFT methods are known to undervalue the gap of bulk diamond (Willey *et al*., 2006) which is in favor of DFT methods that overvalue the C-adamantane gap such as B3LYP. The value of the gap using LSDA theory and advanced (cc-pV (T+d) Z) basis set is 6.472 eV. The comparison of this value with the experimental value of C-adamantane 6.492 eV show that LSDA method is nearer to the experimental value. This value might be as a result of canceling different errors in different directions such as ion relaxation upon excitation and the effect of non-convergent basis set. Hybrid functionals such as B3LYP might perform better than LSDA after adding suitable corrections. However, at the present level of calculations, LSDA seems to be our choice. Most theories (that include present molecular orbital calculations) have some margin of error even the best ones. The present theory and basis seem to be the best fit to the experimental values. Some published papers use the modest theories to be able to have an estimation of computationally demanding physical properties. We hope that, we can improve upon the present research results by using better DFT functionals that require the use of excited states contributions and more powerful basis sets.

IR, Raman, NMR and UV-Vis spectra of AlP diamondoid molecules are computed in the present research. The scale factor of frequencies of vibrational spectra that is used to correlate to experimental values is 0.984. This factor is recommended to current theory and basis (LSDA/6-31G). Our calculations also include ^{1}H-NMR shielding and UV-Vis spectra. UV-Vis is calculated using excited state energy calculations including 40 states with the Time-Dependent Density Functional Theory (TD-DFT) method. Natural Bond Orbital (NBO) population analysis is used in the present research to compare with ideal sp3 hybridized in diamond. All results are achieved using Gaussian 09 package.

RESULTS AND DISCUSSION

Figure 1 illustrates the energy gap change with the total sum of Al and P atoms as expected by current calculations. Figure 1 also shows the energy of Highest Occupied Molecular Orbital (HOMO) and Lowest Unoccupied Molecular Orbital (LUMO). The dotted line denotes the experimental bulk gap of AlP at 2.5 eV (Casey Jr. and Panish, 1978). The fluctuating values of the gap are due to shape effect. Fluctuations are anticipated because of the non-spherical shape of AlP diamondoids (Abdulsattar *et al*., 2013; Abdulsattar and Mohammed, 2014). Diamondoids structure blocks can be organized in numerous classes of shapes.

Figure 2 shows the binding energy of computed AlP diamondoids as a function of the sum of Al and P atoms compared with the bulk amount at 2.5 eV (Causa and Zupan, 1994). For first structures, the binding energy atoms as expected by our DFT results. HOMO and LUMO molecular orbitals are presented. The experimental bulk gap at 2.5 eV (Casey Jr. and Panish, 1978) is shown.

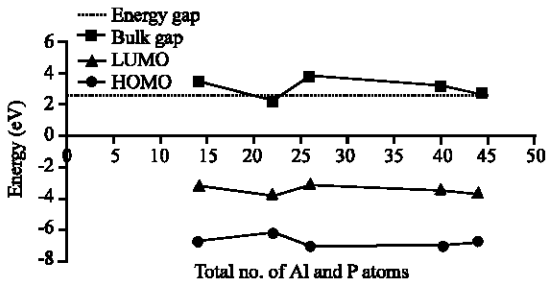

Fig. 1: Energy gap change with the total sum of Al and P atoms as expected by our DFT results. HOMO and LUMO molecular orbitals are presented. The experimental bulk gap at 2.5 eV (Casey Jr. and Panish, 1978)

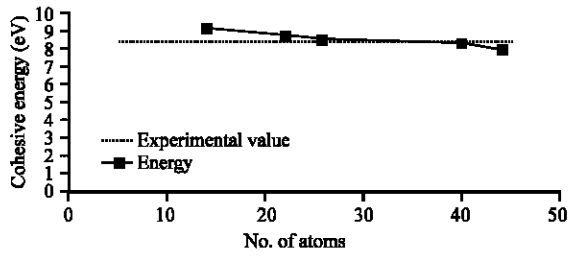

Fig. 2: The relation among the cohesive energy and the sum of Al and P atoms

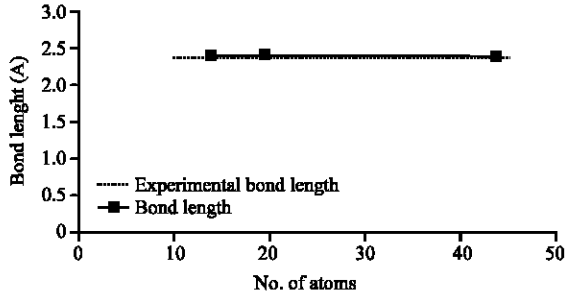

Fig. 3: The bond length as a function of the sum of Al and P atoms. The dashed line represents the experimental value

Figure 2 shows the binding energy of computed AlP diamondoids as a function of the sum of Al and P atoms compared with the bulk amount at 2.5 eV (Causa and Zupan, 1994). For first structures, the binding energy surpasses that of bulk owing to the influence of surface H keen bonds. As the sum of total atoms increases, this effect reduces and the binding energy become nearly constant somewhat inferior to the experimental value.

Figure 3 shows the relation between the bond length of aluminum phosphide molecular core (Al-P) and the sum of core atoms. Also, the Fig. 3 shows that bond length decreases with increasing total sum of Al and P atoms. The bond length decreased from (2.386 Å) for the ($Al_7P_7H_{20}$) molecule to (2.373 Å) for ($Al_{22}P_{22}H_{42}$). Figure 3 is obtained by energy minimization of the investigated molecules. The converged bond length for a high number of core atoms (2.373 Å) is in good agreement with the experimentally reported value (2.36 Å) for bulk AlP (Froyen and Cohen, 1983; Ahmed *et al*., 2008). There is a linear relation between the bond length and lattice constant in the diamond or zincblende structure, so that, Al-P bond length is equal to $\sqrt{3}/4\alpha$ where α is the lattice constant. As a result, all the discussion concerning the bond length applies automatically to lattice constant.

UV-Vis analysis of certain studied molecules in the current work are shown in Fig. 4. The first two molecules are $Al_7P_7H_{20}$ and $Al_{11}P_{11}H_{28}$. These molecules have higher

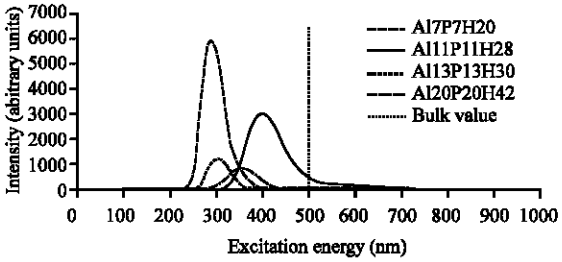

Fig. 4: Change of UV-Vis peaks as a function of excitation energy in nm for AlP diamondoid molecules. The dashed line represents the experimental bulk peak at 496 nm

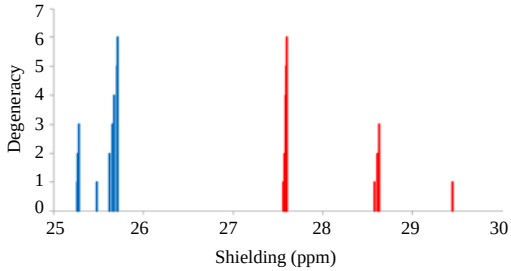

Fig. 5: Nuclear magnetic resonance of AlP diamantane. ^{1}H-NMR lines of Al-H are on the left side (blue) and lines at the right side (red) refer to ^{1}H-NMR spectra of P-H

UV-Vis spectra in comparison with diamondoids structures showed in the same Fig. 5, i.e., AlP hexamantane and octamantane. The cause for this high values is the presence of high ionic polarization charges on $Al_7P_7H_{20}$ and $Al_{11}P_{11}H_{28}$ due to a large number of H atoms with respect to other atoms. The peak maxima in UV-Vis spectra changes from 282 nm for $Al_{11}P_{11}H_{28}$ to 329 nm for AlP octamantane. The following change of values is heading towards bulk experimental 496 nm as suggested by the value of experimental gap 2.5 eV (Casey Jr. and Panish, 1978).

Electronic spin produces shielding to oppose the magnetic field caused by the nucleus. Gauge-Independent Atomic Orbital (GIAO) method is employed in the current NMR computation. Because of symmetry, the first lines of diamantane ($Al_{11}P_{11}H_{28}$) at the left side in Fig. 5 corresponds to ^{1}H-NMR of Al-H and lines at right sides refer to ^{1}H-NMR spectra of P-H. These molecules and other molecules display splitting shielding values that split Al-H shielding to be lower than P-H shielding. This particular behavior is due to the distinct electronegativity between the atoms of the studied system.

Electrostatic forces that bind the molecular system together and the attraction and repulsion between the

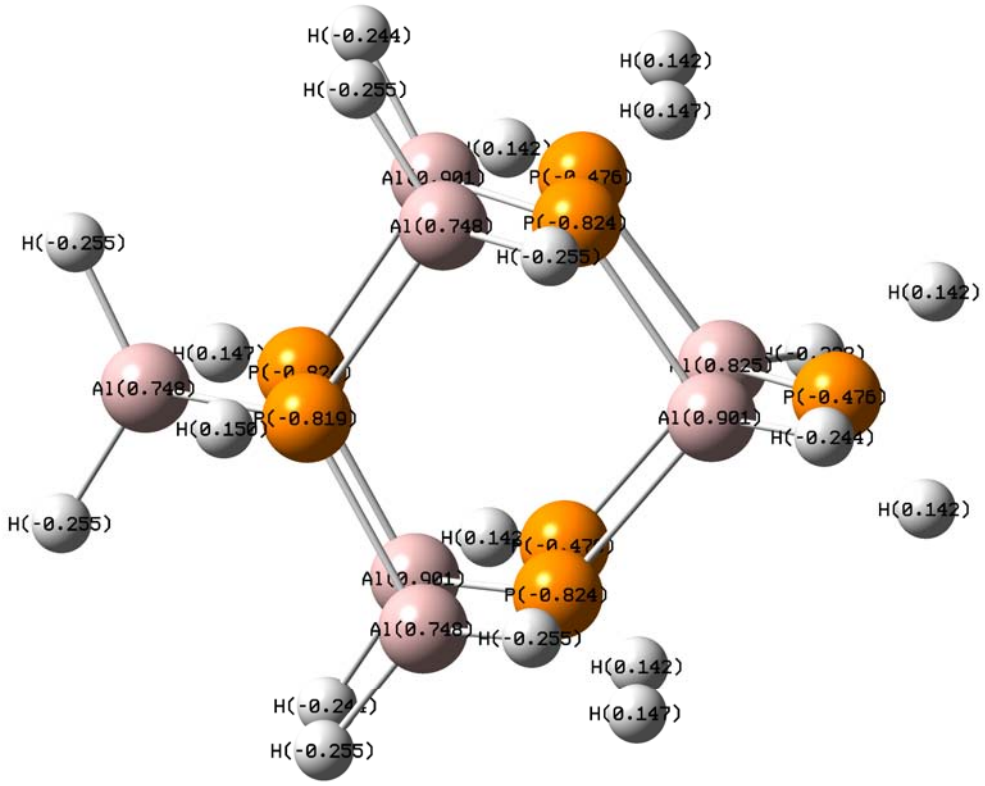

Fig. 6: Distribution of polarization charges on AlP diamantane using Natural Bond Orbital analysis (NBO)

ionic positive and negative polarization charges is shown in Fig. 6 for AlP diamantane. Those forces are working on getting the system stable. This stability condition enables us to study various properties which include nuclear magnetic resonance and the electronic environment around atoms Al, P and H. Al delivers some electronic charge to P and H surface atoms. P has the opposite behavior as we can see from the Natural Bond analysis (NBO) in Fig. 6. The reason for such electron transfer is due to the different electronegativity of constituent atoms.

NBO analysis of hydrogenated AlP diamondoids can be used to investigate the type of bonding between AlP atoms. Current AlP molecules diverge from sp3 bonding that is encountered in carbon diamondoids. Figure 6 shows the distribution of charges according to NBO. From this figure, we can recognize that H atoms that are attached to Al atoms have a negative polarization charge while H atoms that are attached to P atoms have positive polarization charge (Abdulsattar and Al-Bayati, 2007).

Figure 7 shows the IR spectrum of AlP tetramantane using LSDA/3-21G basis sets that can be separated into two different areas depending on the properties of vibration or the gap separation them. The 0-255 cm^{-1} region is characterized by pure Al-P vibrations. The region nearby the broad peak at 615 cm^{-1} has Al-H

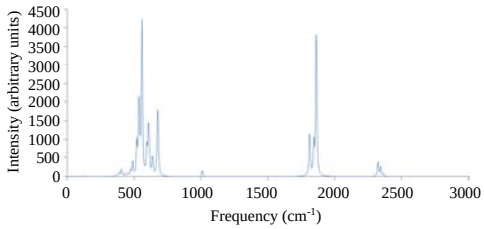

Fig. 7: IR intensity (Epsilon) as a function of the vibration frequency of AlP diamondoid (tetramantane) using LSDA/6-31G

vibrations. There is a noticeable shift in the frequency with an increase in the intensity of the infrared vibrational frequency due to the existence of H surface atoms. This includes the 1736-2390 cm^{-1} mods of Al-H and P-H vibrations that include stretching (symmetric and asymmetric).

Figure 8 shows the Raman spectrum of AlP tetramantane diamondoid structure. It shows that Raman first region is similar to IR but with less activity. The peak intensities in Raman spectrum depend on the probability that a particular wavelength photon will be absorbed. The high-intensity of Raman spectrum is limited in the range 1750-2375 cm^{-1} which is the range of H vibrations.

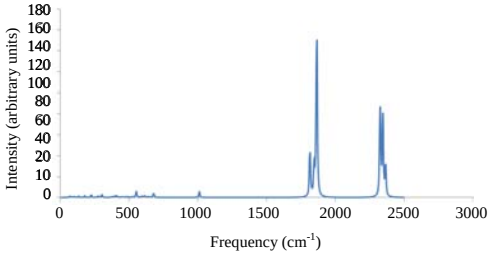

Fig. 8: Raman intensities of AlP diamondoid (tetramantane) as a function of vibration frequency using LSDA/6-31G

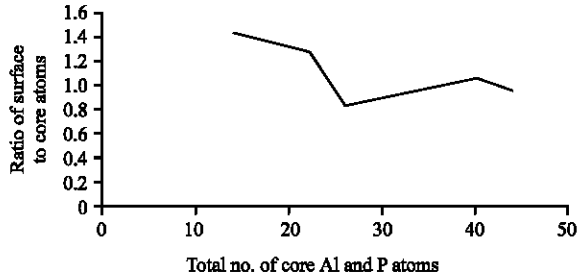

Fig. 9: The ratio of surface H atoms to the sum of core atoms (Al and P) as a function of the sum of core atoms

Finally, Fig. 9 shows the calculated ratio of the surface H atoms to the core atoms. Figure 9 shows that, the highest ratio is equal to 1.42 in diamantane nanocrystal while this ratio began to decrease with increasing the size of crystals with fluctuations in spite of the increase in all of the surface and core atoms. We can note the effect of surface H atoms on many figures such as the values of the energy gap and cohesive energy that have similar behavior to Fig. 9 of the relationship between the surface to core atoms. From this observation, we conclude that the shape of the surface has a direct effect on some properties of studied nanocrystals.

CONCLUSION

The current research illustrates that the energy gap of AlP diamondoid nanocrystals approaches bulk value. As an example, the gap of tetramantane is equal to 2.6 eV which is near the experimental bulk AlP crystal gap at 2.5 eV.

The bond length of all structures of AlP molecules slightly decreased with increasing the number of atoms, and the average cohesive energy decreases with respect to the increase of the size of structures. This decrease is toward approaching experimental values

AlP diamondoids have properties that include: relatively compact structure and stability. ^{1}H-NMR shielding is split in which Al-H shielding is lesser than P-H shielding. Vibrational frequencies (IR and Raman) of diamondoids are divided into two regions. The first region is categorized by nearly pure Al-P vibrations. The second region is characterized by two kinds of vibrations (Al-H and P-H).

The ratio of surface to core atoms decreases with increasing the size of molecules with shape fluctuations. This ratio affects some of the physical properties of diamondoids.

REFERENCES

Abdulsattar, M.A. and I.S. Mohammed, 2014. Diamondoids and large unit cell method as building blocks of InAs Nanocrystals: A density functional theory study. Comput. Mater. Sci., 91: 11-14.

Abdulsattar, M.A. and K.H. Al-Bayati, 2007. Corrections and parametrization of semiempirical large unit cell method for covalent semiconductors. Phys. Rev. B., Vol. 75, https://journals.aps.org/prb/abstract/10.1103/PhysRevB.75.245201.

Abdulsattar, M.A., T.R. Sultan and A.M. Saeed, 2013. Shape and size dependence of electronic properties of InSb diamondoids and nanocrystals: A density functional theory study. Adv. Condens. Matter Phys., Vol. 2013,

Ahmed, R., S.J. Hashemifar and H. Akbarzadeh, 2008. First-principles study of the structural and electronic properties of III-phosphides. Phys. B. Condensed Matter, 403: 1876-1881.

Annane, F., H. Meradji, S. Ghemid and F. El Haj Hassan, 2010. First principle investigation of AlAs and AlP compounds and ordered AlAs1-xPx alloys. Comput. Mater. Sci., 50: 274-278.

Casey Jr. H.C. and M.B. Panish, 1978. Heterostructure Lasers Part A. 1ST Edn., Academic Press, New York, USA, ISBN:9780323157698, Pages: 286.

Causa, M. and A. Zupan, 1994. Density functional LCAO calculation of periodic systems: A posteriori correction of the Hartree-Fock energy of covalent and ionic crystals. Chem. Phys. Lett., 220: 145-153.

Froyen, S. and M.L. Cohen, 1983. Structural properties of III-V Zinc-blende semiconductors under pressure. Phys. Rev. B., 28: 3258-3265.

Jensen, F., 2002. Polarization consistent basis sets II: Estimating the Kohn-Sham basis set limit. J. Chem. Phys., 116: 7372-7379.

Jivani, A.R., H.J. Trivedi, P.N. Gajjar and A.R. Jani, 2005. Total energy, equation of state and bulk modulus of AlP, AlAs and AlSb semiconductors. J. Phy. Pramana, 64: 153-158.

Kim, M.C., E. Sim and K. Burke, 2011. Communication: Avoiding unbound anions in density functional calculations. Chem. Phys., 134: 171103-171103.

Kohanoff, J. and N.I. Gidopoulos, 2003. Density functional theory: Basics, new trends and applications. Handb. Mol. Phys. Quantum Chem., 2: 532-568.

Mujica, A., A. Rubio, A. Munoz and R.J. Needs, 2003. High-pressure phases of group-IV, III-V and II-VI compounds. Rev. Mod. Phys., 75: 863-912.

Mujica, A., P. Rodriguez-Hernandez, S. Radescu, R.J. Needs and A. Munoz, 1999. AIX(X = As, P, Sb) compounds under pressure. Phys. Status Solidi B., 211: 39-43.

Robert, G.P., and Y. Weitao, 1994. Density-Functional Theory of Atoms and Molecules. Oxford University Press, New York, USA., Pages: 332.

Shishkin, M. and G. Kresse, 2007. Self-consistent GW calculations for semiconductors and insulators. Phys. Rev. B., Vol. 75.

Valone, S.M., 2010. Quantal density functional theory II: Approximation methods and applications. J. Am. Chem. Soc., 132: 11387-11388.

Vurgaftman, I., J.A. Meyer and L.A. Ram-Mohan, 2001. Band parameters for III-V compound semiconductors and their alloys. J. Appl. Phys., 89: 5815-5875.

Willey, T.M., C. Bostedt, T.V. Buuren, J.E. Dahl and S.G. Liu *et al*., 2006. Observation of quantum confinement in the occupied states of diamond clusters. Phys. Rev. B., Vol. 74, 10.1103/PhysRevB. 74.205432.